SUPPLEMENTARY MATERIAL

Thiolate end-group regulates ligand arrangement, hydration and affinity for small compounds in monolayer protected gold nanoparticles

Elena Pellizzoni,[a] Maria Şologan,[a] Mario Daka,[a] Paolo Pengo,[a] Domenico Marson,[b] Zbyšek Posel,[b,c] Stefano Franchi,[d] Luca Bignardi,[e] Paola Franchi,[f] Marco Lucarini,[f,] Paola Posocco,[b,*] and Lucia Pasquato[a,*]*

[a] Department of Chemical and Pharmaceutical Sciences and INSTM Trieste Research Unit, University of Trieste, 34127 Trieste (Italy)
[b] Department of Engineering and Architecture, University of Trieste, 34127 Trieste (Italy)
[c] Department of Informatics, Jan Evangelista Purkyně University, 400 96 Ústí nad Labem (Czech Republic)
[d] Elettra Sincrotrone Trieste S.C.p.A., 34149 Trieste (Italy)
[e] Department of Physics, University of Trieste, 34127 Trieste (Italy)
[f] Department of Chemistry "G. Ciamician", University of Bologna, I-40126 Bologna (Italy)

INDEX

1. Additional computational and experimental results

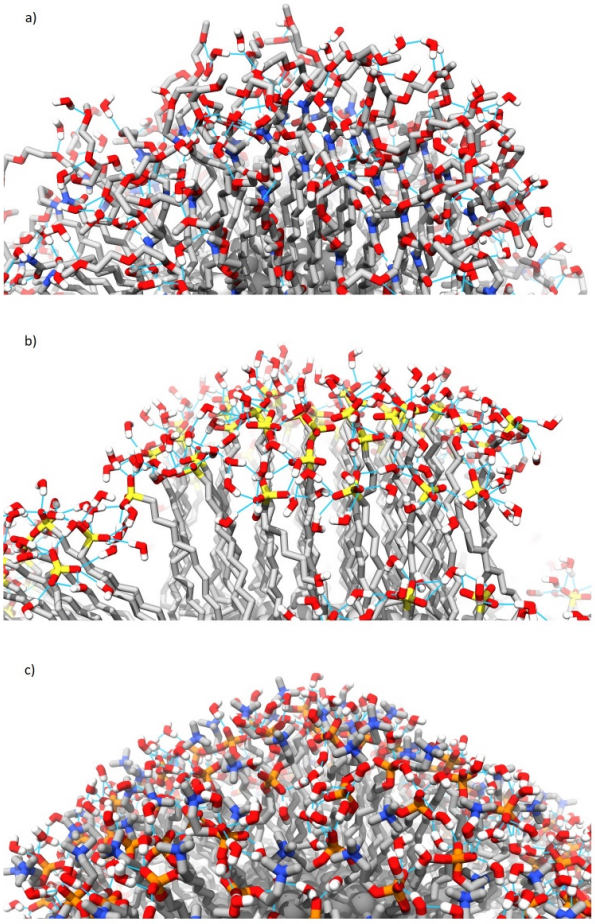

Figure S1. Network of hydrogen bonds inter-ligands and between ligands and water in the monolayer of **NP6**, **NP3**, and **NP5**. Color legend: carbon, grey; oxygen, red; hydrogen, white; sulfur, yellow; phosphorous, orange; nitrogen, blue.

Table S1. Average number of ligand/ligand, ligand/water and ligand/water/ligand hydrogen bonds.

System	Ligand-ligand	Ligand-water	Ligand-water-ligand
NP6	84 ± 7	469 ± 18	45 ± 6
NP3	-	1228 ± 31	201 ± 13
NP4	-	1189 ± 30	188 ± 12
NP5	-	1397 ± 19	240 ± 12

Table S2. Structural properties in water for NP1-6, including: nanoparticle radius of gyration (R_g); average number of ligand bundles; asphericity (δ) and relative ratio of the principal moments of inertia (I_z/I_x, I_z/I_y); fraction of *trans* dihedrals angles. Uncertainties are reported in brackets.

	R_g (nm)	Average number of bundles[a]	δ[b] (-)	I_z/I_x[b] (-)	I_z/I_y[b] (-)	Fraction of *trans* dihedrals (%)[c]
NP1	3.16 (0.02)	no bundles	0.08 (0.03)	1.03 (0.01)	1.02 (0.01)	90.6 (3.0)
NP2	3.15 (0.05)	no bundles	0.13 (0.04)	1.05 (0.02)	1.03 (0.01)	88.5 (6.1)
NP3	3.03 (0.02)	7	0.21 (0.04)	1.12 (0.02)	1.03 (0.01)	95.8 (2.3)
NP4	3.23 (0.06)	5	0.53 (0.05)	1.30 (0.02)	1.05 (0.02)	95.5 (2.7)
NP5	3.21 (0.03)	no bundles	0.14 (0.04)	1.06 (0.01)	1.03 (0.01)	87.7 (2.5)
NP6	2.66 (0.09)	no bundles	0.33 (0.12)	1.21 (0.08)	1.09 (0.05)	90.0 (2.5)

[a] Ligands are assigned to the same bundle based on their relative orientation and end group distances; the Hierarchical Density-based Spatial Clustering of Applications with Noise (HBDSCAN)[1] algorithm was used to identify sets of ligands that belong to the same bundle. We assigned a minimum number of 5 ligands to form a bundle.

[b] The asphericity δ gives an indication of shape and is defined as $I_z-(I_x+I_y)/2$, having defined the principal moments of the gyration tensor as $I_z \geq I_y \geq I_x$. Values close to 0 indicate a spherical form, while values around 1 an oblong shape (e.g., ellipsoid).

[c] The percentage of *trans* dihedrals angles ($-180° < \varphi < -120°$ and $120° < \varphi < 180°$) relative to the total number of dihedral angles in the ligand chain is a measure of ligand ordering. The dihedral angles were calculated taking into account all the heavy atoms of the alkyl portion and ignoring all the hydrogen atoms.

[1] R. J. G. B. Campello; D. Moulavi; J. Sander, In *Density-Based Clustering Based on Hierarchical Density Estimates*, Berlin, Heidelberg, Springer Berlin Heidelberg: Berlin, Heidelberg, 2013; pp 160-172.

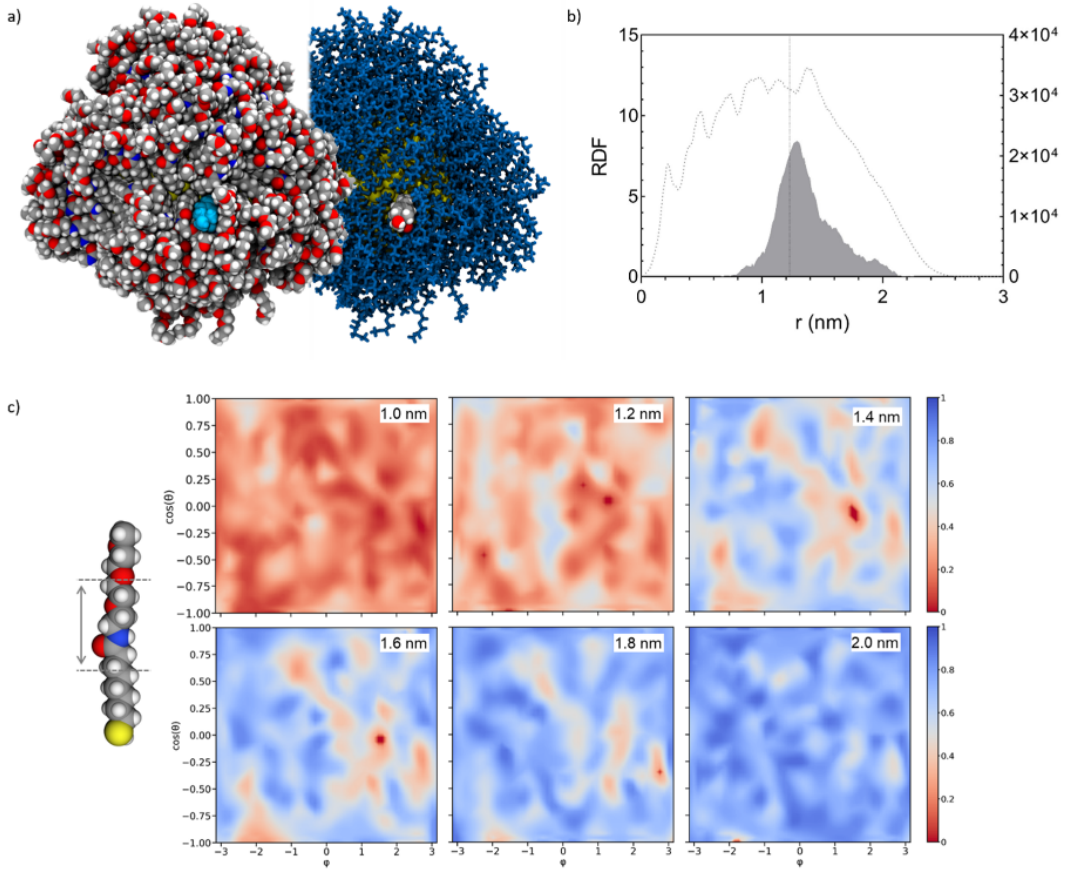

Figure S2. (a) Binding of the radical probe within **NP6** in space-filling model. Solvent is omitted for clarity. Color code: probe, cyan; carbon, grey, nitrogen, blue, oxygen, red; hydrogen, white. The probe is also reported by atomic element (carbon, grey; nitrogen, blue; oxygen, red; hydrogen, white) in the right side of the panel, and the monolayer depicted as blue sticks. (b) Radial distribution function (RDF) of nitrogen atom of the radical probe (solid line, left axis) and ligand (dotted line, right axis) reported from the gold surface. The vertical line highlights the transition between the hydrophobic/hydrophilic portion of the monolayer. (c) Normalized water distribution at increasing distance from the gold surface for **NP6**. The graphs plot the distribution of the atom (oxygen of water or carbon of thiolates) closest to gold surface (centered on the gold core and placed at increasing distances from its surface) shown as a two-dimensional projection of the sphere surface (x-axis, the azimuthal angle φ; y-axis, the cosine of the polar angle θ). Value of 1 indicates that an oxygen atom of a water molecule is always the closest; if it is equal to 0, it indicates that a carbon atom of a chain is always the closest. Simplifying, red to salmon areas represent poorly hydrated zones, while blue areas stand for highly hydrated parts of the monolayer (at a certain distance from the gold surface). The arrow superimposed to the ligand structure helps to identify visually the region within the monolayer which the water maps refer to. At distances lower than those considered the microenvironment is almost hydrophobic, while at higher distances it is fully hydrated and no major difference between the monolayers could be then detected.

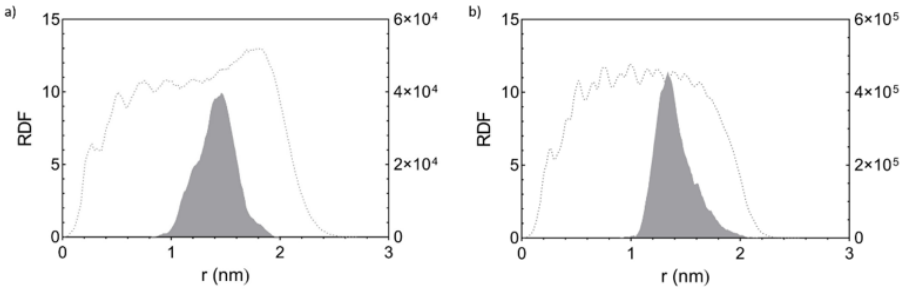

Figure S3. Radial distribution function (RDF) of nitrogen atom of the radical probe (solid line, left axis) and ligand (dotted line, right axis) reported from the gold surface for **NP1** (a) and **NP3** (b).

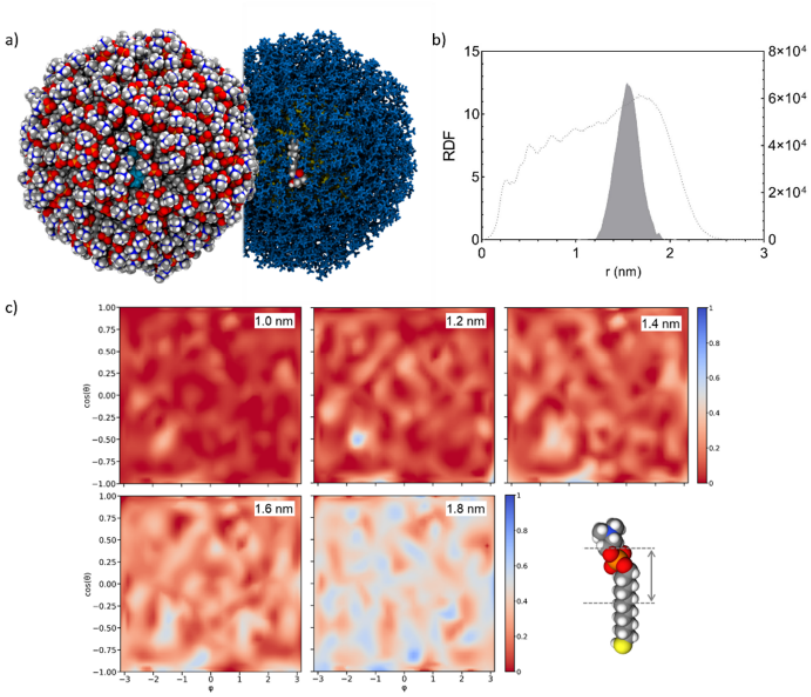

Figure S4. (a) Binding of the radical probe within **NP5** in space-filling model. Solvent is omitted for clarity. Color code: probe, cyan; carbon, grey; nitrogen, blue; oxygen, red; phosphorous, orange; hydrogen, white. The probe is also reported by atomic element (carbon, grey; nitrogen, blue; oxygen, red; hydrogen, white) in the right side of the panel, and the monolayer depicted as blue sticks. (b) Radial distribution function (RDF) of nitrogen atom of the radical probe (solid line, left axis) and ligand (dotted line, right axis) reported from the gold surface. (c) Normalized water distribution at increasing distance from the gold surface for **NP5**. The graphs plot the distribution of the atom (oxygen of water or carbon of thiolates) closest to gold surface (centered on the gold core and placed at increasing distances from its surface) shown as a two-dimensional projection of the sphere surface (x-axis, the azimuthal angle φ; y-axis, the cosine of the polar angle θ). Value of 1 indicates that an oxygen atom of a water molecule is always the closest; if it is equal to 0, it indicates that a carbon atom of a chain is always the closest. Simplifying, red to salmon areas represent poorly hydrated zones, while blue areas stand for highly hydrated parts of the monolayer (at a certain distance from the gold surface). The arrow superimposed to the ligand structure helps to identify visually the region within the monolayer which the water maps refer to. At distances lower than those considered the microenvironment is almost hydrophobic, while at higher distances it is fully hydrated and no major difference between the monolayers could be then detected.

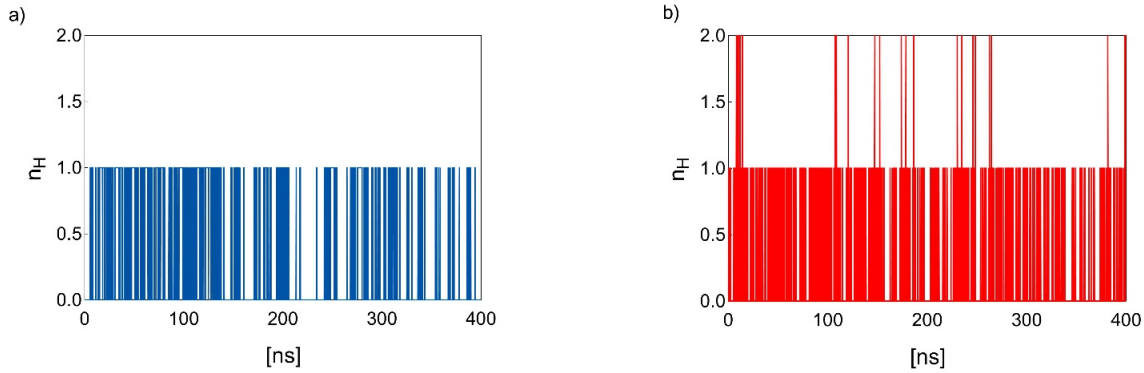

Figure S5. Frequency of ligand-probe hydrogen bonds calculated for **NP5** (a) and **NP6** (b).

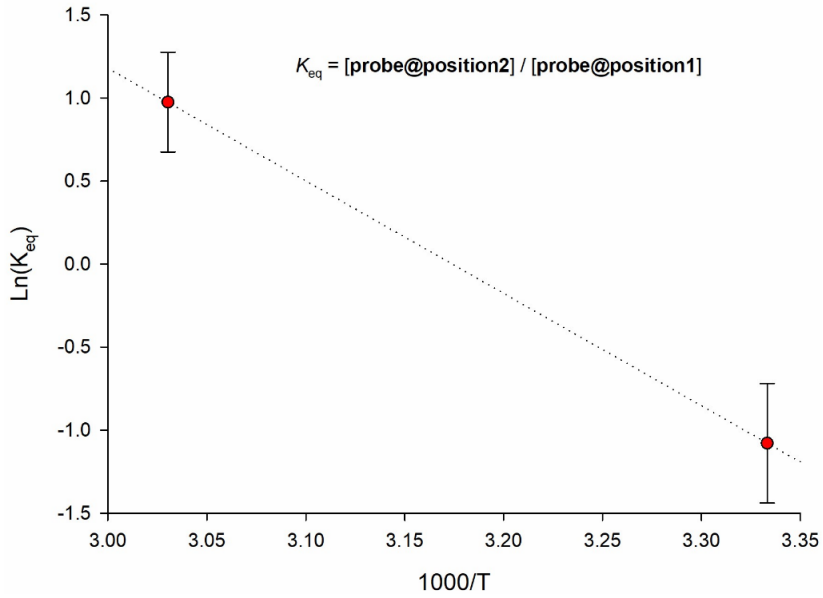

Figure S6. Van't-Hoff plot for the equilibrium **probe@position1** ⇆ **probe@position2** in **NP4**.

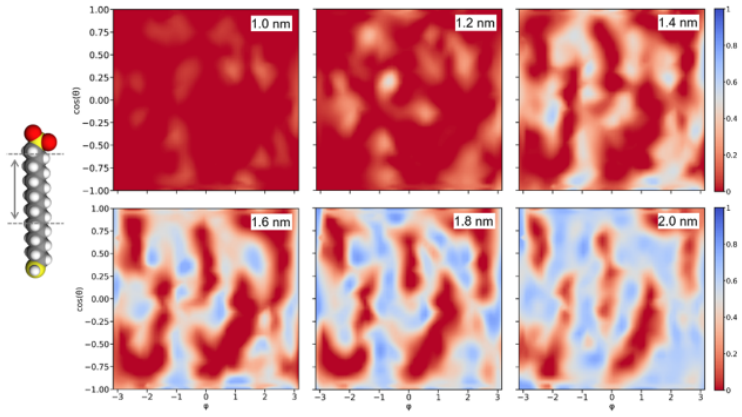

Figure S7. Normalized water distribution at increasing distance from the gold surface for **NP4**. The graphs plot the distribution of the atom (oxygen of water or carbon of thiolates) closest to gold surface (centered on the gold core and placed at increasing distances from its surface) shown as a two-dimensional projection of the sphere surface (x-axis, the azimuthal angle φ; y-axis, the cosine of the polar angle θ). Value of 1 indicates that an oxygen atom of a water molecule is always the closest; if it is equal to 0, it indicates that a carbon atom of a chain is always the closest. Simplifying, red to salmon areas represent poorly hydrated zones, while blue areas stand for highly hydrated parts of the monolayer (at a certain distance from the gold surface). The arrow superimposed to the ligand structure helps to identify visually the region within the monolayer which the water maps refer to. At distances lower than those considered the microenvironment is almost hydrophobic, while at higher distances it is fully hydrated and no major difference between the monolayers could be then detected. For bundled monolayer morphologies as in **NP4**, red areas are mainly constituted by space points belonging to ligand bundles.

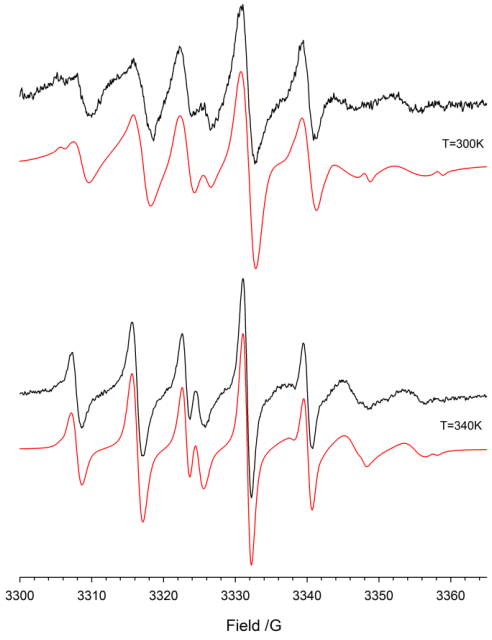

Figure S8. ESR spectra of the radical probe recorded in the presence of **NP2** (14.0 mg/0.1mL) at 300 K (top) and 340 K (bottom). In red are reported the corresponding theoretical simulations obtained by using the spectroscopic parameters reported in Table 1 (main text).

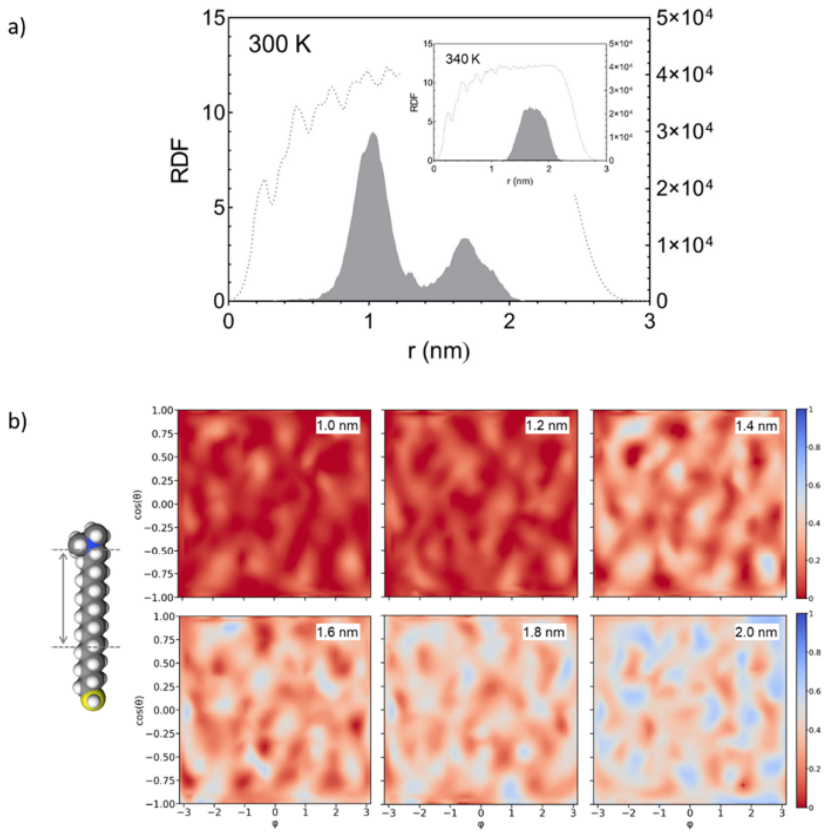

Figure S9. (a) Radial distribution function (RDF) of nitrogen atom of the radical probe (solid line, left axis) and ligand **2** (dotted line, right axis) reported from the gold surface for **NP2**. Insert: RDFs predicted at 340 K. (b) Normalized water distribution at increasing distance from the gold surface for **NP2**. The graphs plot the distribution of the atom (oxygen of water or carbon of thiolates) closest to gold surface (centered on the gold core and placed at increasing distances from its surface) shown as a two-dimensional projection of the sphere surface (x-axis, the azimuthal angle φ; y-axis, the cosine of the polar angle θ). Value of 1 indicates that an oxygen atom of a water molecule is always the closest; if it is equal to 0, it indicates that a carbon atom of a chain is always the closest. Simplifying, red to salmon areas represent poorly hydrated zones, while blue areas stand for highly hydrated parts of the monolayer (at a certain distance from the gold surface). The arrow superimposed to the ligand structure helps to identify visually the region within the monolayer which the water maps refer to. At distances lower than those considered the microenvironment is almost hydrophobic, while at higher distances it is fully hydrated and no major difference between the monolayers could be then detected.

2. Experimental general information

All commercial reagents were purchased from Aldrich and VWR and used without purification unless otherwise mentioned. Solvents were purchased from Aldrich and VWR and deuterated solvents from Cambridge Isotope Laboratories and Aldrich. Dry solvents were obtained from Aldrich. Chlorinated solvents were kept over K_2CO_3 for at least 24 hours prior to use. All other solvents were reagent grade and used as received. Reactions were monitored by TLC on Merck silica gel plates (0.25 mm) and visualized by UV light, I_2, or by $KMnO_4$–H_2SO_4 solution. Chromatography was performed on Merck silica gel 60F-254 (230–400 mesh) and the solvents employed were of analytical grade. NMR spectra were recorded on a Varian 500 spectrometer (operating at 500 MHz for proton, at 125 MHz for carbon), or on a Varian 400 MHz (operating at 400 for proton and at 100.5 MHz for carbon). ^{1}H NMR chemical shifts were referenced to the residual protons in the deuterated solvent. ^{13}C NMR chemical shifts were referenced to the solvent chemical shift. Chemical shifts (δ) are reported in ppm and the multiplicity of each signal is designated by the conventional abbreviations: s, singlet; d, doublet; t, triplet; q, quartet; m, multiplet; br, broad; dd, doublet of doublets. Coupling constants (*J*) are quoted in Hz. UV-Visible spectra were recorded on a Shimadzu UV-1800 spectrophotometer. TGA analyses were performed on TGA Q-500 V6.3 Build 189 using a heating rate of 10 °C min^{-1} up to 1000 °C under N_2 flow. TEM images were obtained with Jeol 3010 high resolution electron microscope (1.7 nm point-to-point) operating at 300 keV using a Gatan slow-scan CCD camera (mod. 794). TEM samples of protected gold nanoparticles were prepared by placing a single drop of 0.5 mg mL^{-1} MeOH or H_2O/iPrOH solution onto a 200-mesh copper grid coated with an amorphous carbon film. NPs gold core diameters were measured manually using Gatan software Digital Micrograph on at least 200 particles.

Electrospray Ionization (ESI) mass analyses were performed on a Perkin Elmer APII at 5600 eV and exact mass analyses on a Bruker Daltonics micrOTOF-Q operating at 3200 V capillary potential.

Radical probe (*para*-*n*-pentyl-benzyl)-1-hydro-2-methyl-2-propylnitroxide was generated by mixing 0.5 μL of a methanol solution containing the corresponding amine (0.1 M) and 0.5 μL of a water solution containing Oxone (0.1 M) with 100 μL of a water solution containing variable amounts of **NP1**-**NP6**. Samples were transferred in capillary tubes (diameter 1 mm) and then placed inside the thermostatted cavity of the EPR spectrometer. ESR spectra were collected using a Bruker ELEXYS spectrometer equipped with an NMR gaussmeter for field calibration. The sample temperature was controlled with a standard variable temperature accessory and monitored before and after each run using a copper-constantan thermocouple. The instrument settings were as follows: microwave power 5.0 mW, modulation amplitude 0.05 mT, modulation frequency 100 kHz, scan time 180 s. Digitized EPR spectra

were transferred to a personal computer for analysis using digital simulations carried out with a program developed in our laboratory and based on a Monte Carlo procedure. DLS measurements have been performed on a Malvern zeta Sizer Nano, using a concentration for the nanoparticles between 0.1 – 0.4 mg/mL in water, scattering angle 173°, 25 °C, disposable cuvettes.

3. Synthesis of ligands

3.1 Synthesis of thiol 2

Thiol **2** was synthesized following the procedure reported in Scheme S1, slightly modify from literature.[2]

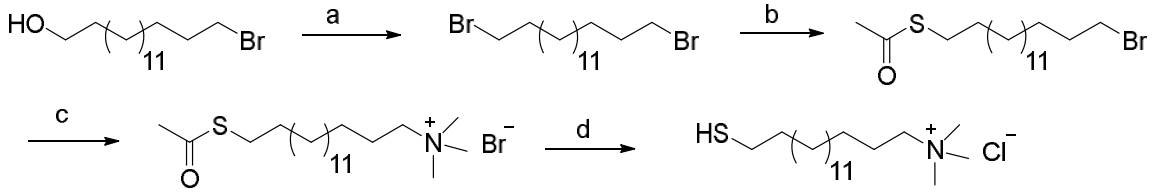

Scheme S1: Synthesis of HS-C16N: a. CBr_4, PPh_3, dry DCM, 48 h, r.t.; b. KSAc, dry THF, 12 h, reflux; c. NMe_3, dry THF, 10 days, r.t.; d. HCl 6M deox, EtOH deox, 2 h, reflux.

Synthesis of 1,16-dibromohexadecane

PPh_3 (1.06 g, 4.06 mmol, 2.6 eq) and CBr_4 (1.24 g, 3.74 mmol, 2.4 eq) were dissolved with 20 mL of anhydrous DCM in a round bottom flask under argon atmosphere. After 5 minutes, 16-bromohexadecan-1-ol (0.5 g, 1.56 mmol, 1 eq) was added. The solution turns from yellow to colorless and after 2h a white precipitate was observed. The reaction was stirred overnight, then the precipitate was filtered off and the product was dried under reduced pressure, coevaporating with diethyl ether in order to remove all the DCM. The resulting white solid was washed with an aqueous solution of ethanol 60% (6 x 100 mL) and after the evaporation of the remaining solvent, 580 mg of white product were obtained. Yield 97%.

^{1}H-NMR (400 MHz, $CDCl_3$) δ: 1.20 ÷ 1.33 (m, 24H, -$\underline{CH_2}$-), 1.41 (m, 4H, -$\underline{CH_2}$-CH_2 -CH_2-Br), 1.85 (m, 4H, -$\underline{CH_2}$- CH_2-Br), 3.40 (t, J = 7.0, 4H, -$\underline{CH_2}$-Br).

^{13}C-NMR (500 MHz, $CDCl_3$) δ: 28.15 (2C, $\underline{CH_2}$- CH_2- CH_2-Br), 28.75, 29.41, 29.44, 29.51, 29.59, 29.61 (10C, -CH_2- $\underline{CH_2}$- CH_2-), 32.82 (2C, -$\underline{CH_2}$- CH_2-Br), 34.04 (2C, -$\underline{CH_2}$-Br).

[2] M. Wu, A. M. Vartanian, G. Chong, A. Kumar Pandiakumar, R. J. Hamers, R. Hernandez, C. J. Murphy *J. Am. Chem. Soc.* **2019**, *141*, 4316-4327.

Synthesis of 16-bromohexadecanthioacetate

0.300 g (0.78 mmol, 2.2 eq) of 1,16-dibromohexadecane were dissolved in 2.16 mL of anhydrous THF and KSAc (0.041 g, 0.35 mmol, 1 Eq) was added at once. The mixture was stirred and refluxed overnight. The solvent was removed under reduced pressure and then purified by gradient flash chromatography eluting with petroleum ether: DCM mixture from 95:5 to 70:30. A white solid was obtained (0.096 g) yield 72%.

^{1}H-NMR (400 MHz, $CDCl_3$) δ: 1.10÷1.45 (m, 24H, $\underline{CH_2}$- CH_2- CH_2-Br and -CH_2- $\underline{CH_2}$- CH_2-), 1.56 (m, 2H, -$\underline{CH_2}$-CH_2-S-$COCH_3$), 1.84 (m, 2H, -$\underline{CH_2}$- CH_2-Br), 2.30 (s, 3H, -S-CO-$\underline{CH_3}$), 2.84 (t, J = 7.4, 2H, -$\underline{CH_2}$-S-$COCH_3$), 3.40 (t, J = 7.0, 2H, -$\underline{CH_2}$-Br).

ESI-MS (m/z): 381 [M+H^+], 403 [M+Na^+]

Synthesis of trimethylamine-hexadecanethioacetate

80 mg (0.21 mmol, 1 eq) of 16-bromohexadecanthioacetate were dissolved in a Pyrex in 3 mL of anhydrous THF. 2 mL (8.4 mmol, 40 eq) of 4.2 M trimethylamine solution in ethanol was added and the mixture was stirred at room temperature for 10 days. After drying under reduced pressure the product was obtained in quantitative yield as a white solid.

^{1}H-NMR (400 MHz, $CDCl_3$) δ: 1.17 - 1.46 (m, 24H, -$\underline{CH_2}$- CH_2- CH_2- $N(CH_3)_3$ and -CH_2- $\underline{CH_2}$- CH_2-), 1.55 (m, 2H, -$\underline{CH_2}$-CH_2-S-$COCH_3$), 1.76 (m, 2H, -$\underline{CH_2}$- CH_2-$N(CH_3)_3$), 2.23 (s, 3H, -S-CO-$\underline{CH_3}$), 2.86 (t, J = 7.4, 2H, -$\underline{CH_2}$-S-$COCH_3$), 3.56 (m, 2H, -CH_2- $N(\underline{CH_3})_3$).

^{13}C-NMR (400 MHz, $CDCl_3$) δ: 23.19 (1C, -$\underline{CH_2}$- CH_2-$N(CH_3)_3$), 26.11 (1C, -$\underline{CH_2}$- CH_2- CH_2- $N(CH_3)_3$), 28.79, 29.07, 29.13, 29.17, 29.29, 29.39, 29.43, 29.47, 29.48, 29.51, 29.53, 29.55, 29.57, 29.58 (14C, -$\underline{CH_2}$- CH_2- CH_2- $N(CH_3)_3$ and -CH_2- $\underline{CH_2}$- CH_2-), 29.15 (1C, -$\underline{CH_2}$-CH_2-S-$COCH_3$), 30.59 (1C, -S-CO-$\underline{CH_3}$), 29.12 (1C, -$\underline{CH_2}$-S-$COCH_3$), 66.94 (1C, CH_2- $N(\underline{CH_3})_3$).

ESI-MS (m/z): 358 [M+]

Synthesis of thiol 2

To a solution of trimethylamine-hexadecanethioacetate (0.085 g, 0.237 mmol) in 1.1 mL EtOH, 0.72 mL of deoxygenated HCl 6 M was added and the solution was let to stir for 3h. The solution was evaporated and the product was obtained in quantitative yield.

^{1}H-NMR (400 MHz, deoxygenated $CDCl_3$) δ: 1.18 ÷1.45 (m, 24H, -$\underline{CH_2}$- CH_2- CH_2- $N(CH_3)_3$ and -CH_2- $\underline{CH_2}$- CH_2-), 1.60 (m, 2H, -$\underline{CH_2}$-CH_2-SH), 1.74 (m, 2H, -$\underline{CH_2}$- CH_2-$N(CH_3)_3$), 2.51 (m, 2H, -$\underline{CH_2}$-SH), 3.43 (s, 9H, -CH_2- $N(\underline{CH_3})_3$), 3.52 (m, 2H, $\underline{CH_2}$- $N(CH_3)_3$).

MS-ESI: m/z calc for $[C_{19}H_{42}NS]^+$ 316.6135, found 316.3031.

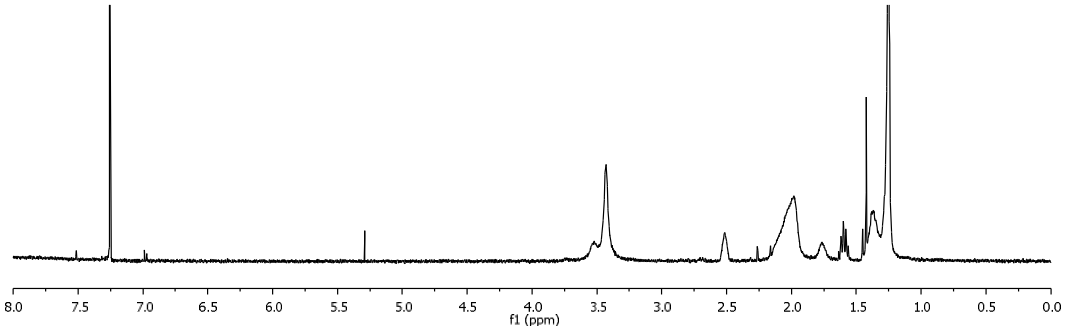

Figure S10. ^{1}H NMR (400 MHz, CD_3OD) spectra of thiol **2**.

3.2 Synthesis of thiol 4

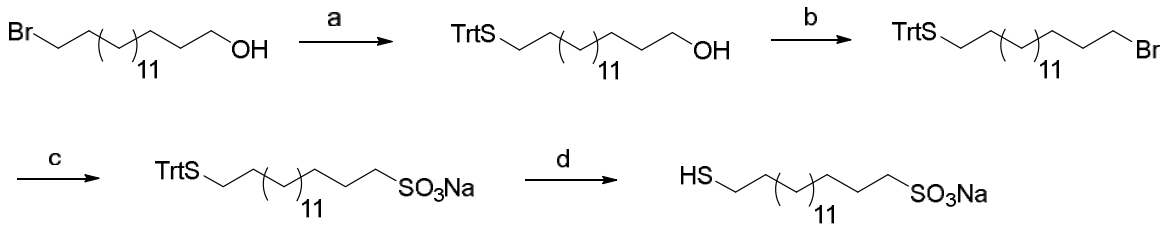

Scheme S2: Synthesis of MHDS: a. TrtSH, K_2CO_3, DMF; b. MsCl, DCM, LiBr, THF; c. Na_2SO_3, microwave; d. TFA, TIPS, DCM.

Synthesis 16-(tritylthio)hexadecan-1-ol

0.500 g (1.55 mmol, 1 eq) of 16-bromohexadecan-1-ol, 0.430 g (1.55 mmol, 1 eq) of triphenylmethanethiol and 0.430 g (3.1 mmol, 2 eq) of potassium carbonate were suspended in 4 mL of anhydrous DMF in a Pyrex tube with a screw cap under flux of argon. The mixture was heated at reflux overnight using an oil bath.

The mixture was filtered to remove carbonate and washed with water (4 x 100 mL) to remove DMF. The resulting organic phase was dried with anhydrous sodium sulfate while the solvent was removed under reduced pressure. 0.695 g of pure product were obtained (orange oil). Yield: 87%.

^{1}H-NMR (400 MHz, $CDCl_3$) δ: 1.26 ÷ 1.17 (m, 22H, CH_2), 1.31 (m, 2H, $\underline{CH_2}CH_2CH_2OH$), 1.37 (m, 2H, $\underline{CH_2}CH_2S$), 1.56 (m, 2H, $\underline{CH_2}CH_2OH$), 2.13 (t, J = 7.4, 2H, $\underline{CH_2}S$), 3.64 (t, J = 6.6, 2H, $\underline{CH_2}OH$), 7.20 (m, 3H, CH Ar. para), 7.27 (m, 6H, CH Ar. meta), 7.41 (m, 6H, CH Ar. ortho).

ESI mass: 539 m/z $[M+Na^+]$.

Synthesis of 16-(tritylthio)hexadecyl 4-methylbenzenesulfonate

In a Pyrex tube, under argon, 0.270 g (1.4 mmol, 1.04 eq) of tosylchloride were dissolved in 1 mL of anhydrous DCM. A solution of 16-(tritylthio)hexadecan-1-ol (0.7 g, 1.34 mmol, 1 eq) and triethylamine (0.270 g, 2.68 mmol, 2 eq, 0.37 mL) in 2 mL of anhydrous DCM was added to the solution of tosylchloride at 0 °C under flux of argon. The resulting solution was stirred for 15 min at 0 °C and overnight at room temperature. The crude product was purified by silica gel flash chromatography eluting with 6:4 DCM : petroleum ether mixture. A colorless oil was obtained as pure product, 0.600 g, yield 66%.

^{1}H-NMR (400 MHz, $CDCl_3$) δ: 1.32 ÷ 1.10 (m, 20H, CH_2), 1.21 (m, 2H, $\underline{CH_2}CH_2CH_2S$), 1.27 (m, 2H, $\underline{CH_2}CH_2CH_2O$), 1.37 (m, 2H, $\underline{CH_2}CH_2S$), 1.62 (m, 2H, $\underline{CH_2}CH_2O$), 2.13 (t, J = 7.3, 2H, $\underline{CH_2}S$), 2.45 (s, 3H, CH_3, Tosyl) 4.02 (t, J = 6.5, 2H, $\underline{CH_2}O$), 7.20 - 7.34 (m, 11H, CH Ar), 7.41 (m, 6H, CH), 7.79 (m, 2H, CH Ar).

^{13}C-NMR (400 MHz, $CDCl_3$) δ: 21.6 (1C, CH_3 Ts), 25.31 (1C, CH_2, $\underline{CH_2}CH_2CH_2O$), 28.53 (1C, CH_2 $\underline{CH_2}CH_2S$), 28.78 (1C, $CH_2\underline{CH_2}CH_2O$), 28.92 (1C, CH_2), 29.00 (1C, CH_2), 29.18 (1C, CH_2), 29.37 (1C, CH_2), 29.41 (1C, CH_2), 29.49 (1C, CH_2), 29.55 (1C, CH_2), 29.59 (1C, CH_2), 29.61 (1C, CH_2), 29.62 (1C, CH_2), 29.63 (1C, CH_2), 32.06 (1C, CH_2, $\underline{CH_2}S$), 70.67 (1C, CH_2, $\underline{CH_2}O$).

Synthesis of (16-bromohexadecyl)(trityl)sulfane

0.590 g (0.89 mmol, 1 equiv) of 16-(tritylthio)hexadecyl 4-methylbenzenesulfonate were dissolved in 17 mL of deoxygenated acetone in a Pyrex tube with a screw cap. To this solution, 0.230 g (2.67 mmol, 3 Eq) of LiBr were added and the clear colorless solution was stirred at reflux for 3 hours. A white precipitate was obtained. The mixture was diluted with a saturated solution of $NaHCO_3$ and the product was extracted with DCM (5 x 30 mL). The organic phase was dried with anhydrous sodium sulfate, the solvent was removed under reduced pressure to obtain the pure product (0.510 g, yield 87%).

^{1}H-NMR (400 MHz, $CDCl_3$) δ: 1.11 ÷ 1.32 (m, 24H, CH_2), 1.39 (m, 2H, $\underline{CH_2}CH_2S$), 1.85 (m, 2H, $\underline{CH_2}CH_2Br$), 2.13 (t, J = 7.3, 2H, $\underline{CH_2}S$), 3.4 (t, J = 6.9, 2H, $\underline{CH_2}Br$), 7.20 (m, 3H, *para*-CH Ar), 7.28 (m, 6H, *meta*-CH Ar), 7.41 (m, 6H, *ortho*-CH Ar).

Synthesis of 16-(tritylthio)hexadecane-1-sulfonate

0.149 g (0.26 mmol, 1 equiv) of 16-bromohexadecyl)(trityl)sulfane and 0.051 g (0.41 mmol, 1.6 equiv) of Na_2SO_3 were suspended in 2 mL of 1:2:2 THF : ethanol : water mixture in a microwave tube and four cycles were performed heating at 140°C for 15 min. The obtained mixture was dried under vacuum and

washed by decantation with diethyl ether (6 x 15 mL). The crude was suspended in ethanol (4 x 20 mL), heated at reflux for 5 min and filtered under reduced pressure. The obtained clear solution was dried under reduced pressure to give 0.093 g of white solid pure product, yield 60%.

^{1}H-NMR (400 MHz, $CDCl_3$) δ: 1.11 ÷ 1.32 (m, 22H, CH_2), 1.35 (m, 2H, $\underline{CH_2}CH_2S$), 1.40 (m, 2H, $\underline{CH_2}CH_2CH_2SO_3^-$), 1.78 (m, 2H, $\underline{CH_2}CH_2SO_3^-$), 2.12 (t, J = 7.3, 2H, $\underline{CH_2}S$), 2.77 (m, 2H, $\underline{CH_2}SO^-_3$), 7.20 (m, 3H, *para*-CH Ar), 7.27 (m, 6H, *meta*-CH Ar), 7.38 (m, 6H, *ortho*-CH Ar).

ESI mass: 579 m/z [M^+]. Exact Mass calc. for $C_{35}H_{47}O_3S_2$ 579.2972; found: 579.2961.

Synthesis of 16-mercaptohexadecane-1-sulfonate (4)

In a round bottom flask of 10 mL with a stirring bar and under flux of argon, 0.045 mg (0.075 mmol, 1 eq) of 16-(tritylthio)hexadecane-1-sulfonate were suspended in 830 µL of deoxygenated DCM. 115 µL (171 mg, 1.5 mmol, 20 equiv) of TFA and 37 µL (28.5 mg, 0.18 mmol, 2.4 eq) were sequentially added and the mixture was stirred for 3 h under argon at room temperature.

After this time the mixture was dried under flux of argon and the excess of TFA was removed by addition of deoxygenated methanol (2 x 1 mL) and removal of it under flux of argon. The crude was washed with deoxygenated hexane (10 x 6 mL) by decantation. After drying under flux of argon, a white pure product was obtained, quantitative yield.

^{1}H-NMR (400 MHz, CD_3OD) δ: 1.25 ÷ 1.46 (m, 24H, CH_2), 1.57 (m, 2H, $\underline{CH_2}CH_2SH$), 1.78 (m, 2H, $\underline{CH_2}CH_2SO_3^-$), 2.48 (m, 2H, $\underline{CH_2}SH$), 2.77 (m, 2H, $\underline{CH_2}SO^-_3$).

ESI mass: 337 m/z [M^+].

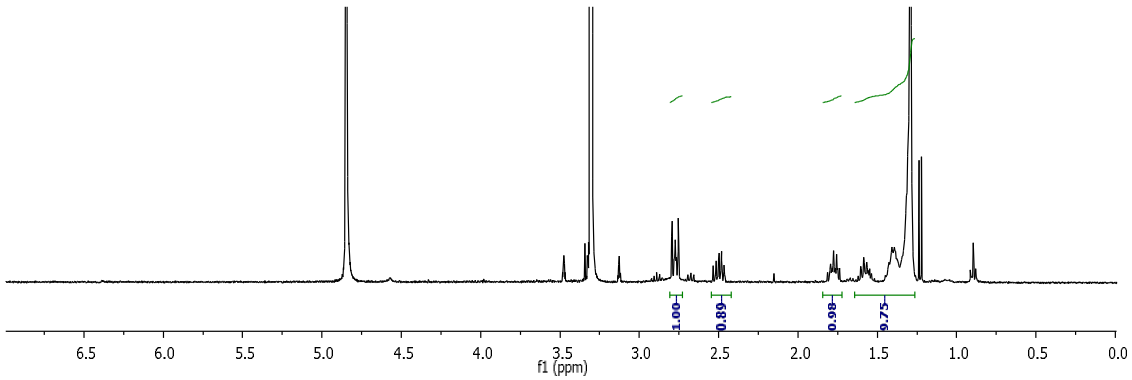

Figure S11. ^{1}H-NMR (400 MHz, CD_3OD) spectrum of thiol **4**.

3.3 Synthesis of thiol 5

The synthesis was carried out with a modification to the procedure reported in the literature.[3]

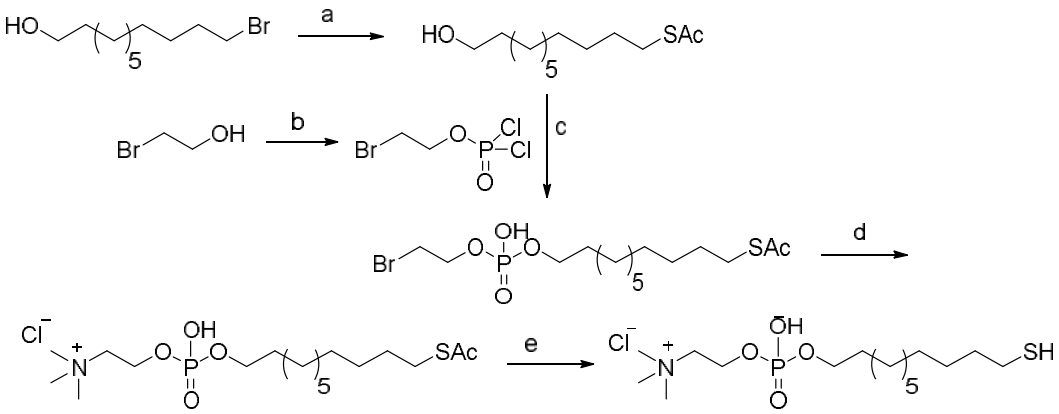

Scheme S3: a. KSAc, THF, overnight; b. $POCl_3$, DCM, 17 h; c. Et_3N, THF, 22 h; d. NMe_3, THF, 72h; e. EtOH, HCl, 2 h.

Synthesis of 2-bromoethyl fosforodichlorohydrate

5.000 g of 2-bromoethanol ($40.0 \cdot 10^{-3}$ moles, 1 eq) were added to a solution of 11.000 g of $POCl_3$ ($71.7 \cdot 10^{-3}$ moles, 1.75 eq) and 6.0 mL of dichloromethane in 5 minutes at room temperature. The solution was let to stir for 19 h and the solvent was evaporated giving 9.758 g ($40.0 \cdot 10^{-3}$ moles) of a brown oil in quantitative yield.

^{1}H-NMR (500 MHz, $CDCl_3$) δ: 4.58 (dt, J = 10.5, 6.4 Hz, 2H, C$\underline{H_2}$-$OPOCl_2$), 3.92 (t, J = 5.4, 0.08 H, C$\underline{H_2}$-OH), 3.61 (td, J = 6.3, 0.7, 2H, Br-C$\underline{H_2}$).

Synthesis of 11-hydroxy-undecyl-ethantioate

To a solution of 6.783 g of 11-bromo-1-undecanol ($27 \cdot 10^{-3}$ moles, 1 eq) in 40.0 mL of anhydrous DMF, 3.084 g of potassium tioacetate ($27 \cdot 10^{-3}$ moles, 1 eq) were added and the solution was let to stir for 1h. Then 30 mL of diethyl ether/water were added in order to precipitate all the potassium bromide. The as-resulting dispersion was washed with water (5 x 20 mL) and the organic phase was evaporated giving 6.091 g ($24.7 \cdot 10^{-3}$ moles) of a white solid. Yield: 91.4 %.

^{1}H-NMR (400 MHz, $CDCl_3$) δ: 3.63 (t, J = 6.6, 2H, C$\underline{H_2}$-OH), 2.85 (t, J = 7.36, 2H, CH_3COS- C$\underline{H_2}$), 2.31 (s, 3H, C$\underline{H_3}$COS), 1.60 – 1.50 (m, 5H, CH_2-C$\underline{H_2}$-CH_2), 1.39 – 1.23 (m, 16H, CH_2-C$\underline{H_2}$-CH_2).

[3] R. E. Holmlin, X. Chen, R. G. Chapman, S. Takayama, G. M. Whitesides *Langmuir*, **2001**, *17*, 2841-2850.

Synthesis of 11-(tioacetyl)undecyl-2-bromoethyl-hydrogenfosfate

A solution of 8.782 g di 11-*S*-acetil-1-undecanol ($24.2 \cdot 10^{-3}$ moles, 1 eq) and 3.673 g of trimethylamine (5.1 mL, $36.3 \cdot 10^{-3}$ moles, 1.5 eq) in 100 mL of anhydrous THF was added to a solution of 2-bromoethyl phosphorus dichlorohydrate (5.963, $36.3 \cdot 10^{-3}$ moles, 1.5 eq) and let to stir for 22 h. Then 250 mL of toluene were added, the dispersion was filtrated and the solvent was removed. To the solid 500 mL of THF and 500 mL of $NaHCO_3$ 0.5 M were added and the solution let to stir for other 22 h. The solution was acidified to pH 3 using sulfuric acid and the organic phase was extracted with diethyl ether (4 x 200 mL). The organic phase was separated and the solvent was removed giving 9.949 g ($22.96 \cdot 10^{-3}$ moles) of a yellowish solid. Yield: 94.9 %.

^{1}H-NMR (500 MHz, $CDCl_3$) δ: 4.40 – 4.18 (m, 2H, PO-C$\underline{H_2}$-CH_2Br), 4.09 – 4.01 (m, 2H, CH_2-C$\underline{H_2}$-OP), 3.54 (dt, *J* = 12.8, 6.2, 2H, POCH_2-C$\underline{H_2}$-Br), 2.85 (t, *J* = 7.4, 2H, CH_3COS-C$\underline{H_2}$- CH_2), 2.31 (s, 3H, C$\underline{H_3}$COS), 1.74 – 1.63 (m, 2H, CH_2-C$\underline{H_2}$- CH_2OP), 1.59 – 1.50 (m, 2H, CH_3COS-CH_2-C$\underline{H_2}$- CH_2), 1.41 – 1.19 (m, 15H, CH_2-C$\underline{H_2}$- CH_2).

Synthesis of 11-(tioacetyl)undecyl-(2-(trimethylammonium)ethyl)fosfate

11.5 mL of a solution of trimethylamine (43% in H_2O) was added to a solution of 1.521 g of 11-(tioacetyl)undecyl-2-bromoethyl-hydrogenfosfate ($3.51 \cdot 10^{-3}$ moles, 1 eq) in 30 mL THF. The mixture was let to stir for 3 days and after the evaporation of the solvent the product was purified using flash chromatography giving 0.800 g ($1.94 \cdot 10^{-3}$ mol) of the product. Yield: 55.27 %.

^{1}H-NMR (400 MHz, $CDCl_3$) δ: 4.33 (br. s, 2H, PO-C$\underline{H_2}$-CH_2NMe_3), 3.95 (br s, 2H, CH_2-C$\underline{H_2}$-OP), 3.83 (br s, 2H, POCH_2-C$\underline{H_2}$-NMe_3), 3.45 (br, s, 9H, NMe_3), 2.30 (s, 3H, C$\underline{H_3}$-COS), 1.62 – 1.47 (m, 4H, CH_2-C$\underline{H_2}$- CH_2OP, CH_3COSCH_2-C$\underline{H_2}$- CH_2), 1.24 (s, 15H, CH_2-C$\underline{H_2}$- CH_2).

Synthesis of thiol 5

To a solution of 0.025 g (0.06 mmol) of 11-(tioacetyl)undecyl-(2-(trimethylammonium)ethyl)fosfate dissolved in 2 mL ethanol, 2 mL of HCl 6 M were added and the mixture was let to stir at 78 °C for 2h. After this time the solvent was evaporated and 45 mg of a white solid was obtained. Quantitavie yield.

^{1}H-NMR (400 MHz, CD_3OD) δ: 4.45 (m, 2H, PO-C$\underline{H_2}$-CH_2NMe_3), 4.05 (m, 2H, POCH_2-C$\underline{H_2}$-NMe_3), 3.75 (m, 2H, CH_2-C$\underline{H_2}$-OP), 3.23 (br, s, 9H, N(C$\underline{H_3}$)$_3$), 2.5 (t, *J* = 7.1, 2H, CH_2-S), 1.7 – 1.3 (m, 19H, CH_2-C$\underline{H_2}$).

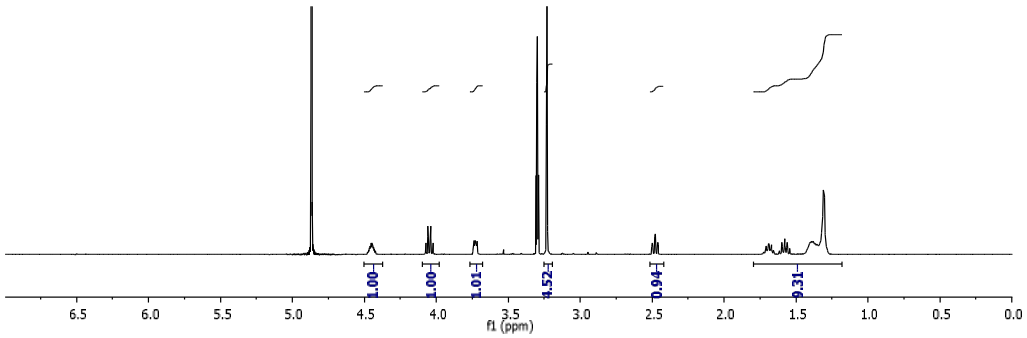

Figure S12. ^{1}H NMR (400 MHz, CD_3OD) spectra of thiol **5**.

4. Characterization of monolayer protected gold nanoparticles

4.1 Characterization of NP1

a)

b)

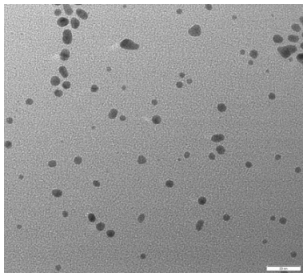

Scale bar = 20 nm

c)

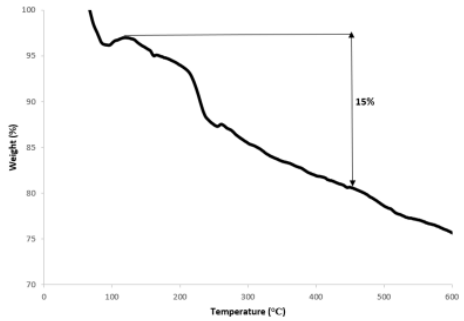

d)

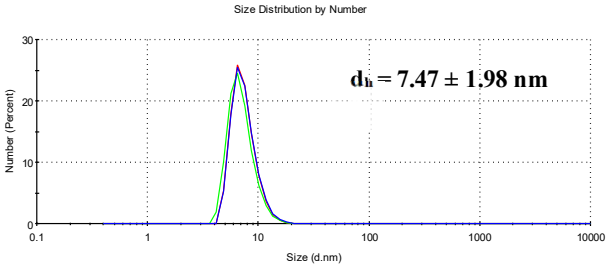

Figure S13. a) Size histogram and b) representative TEM image; c) TGA and d) hydrodynamic diameter size distribution ± std, n = 3, determined by DLS of **NP1**.

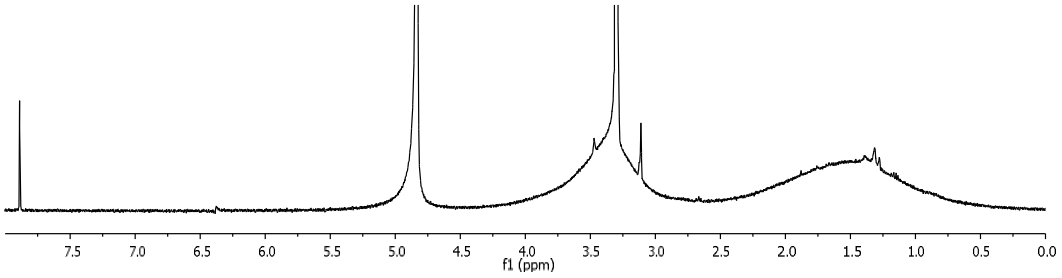

Figure S14. ^{1}H-NMR (400 MHz, CD_3OD) spectrum of **NP1**.

4.2 Characterization of NP2

a)

b)

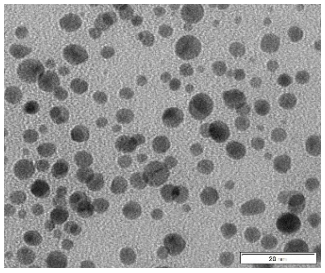

Scale bar: 20 nm

c)

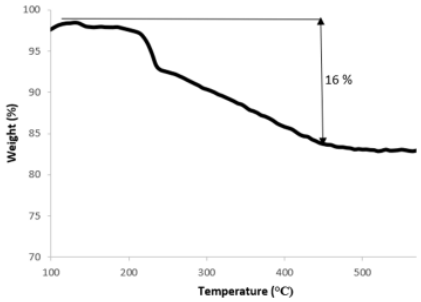

d)

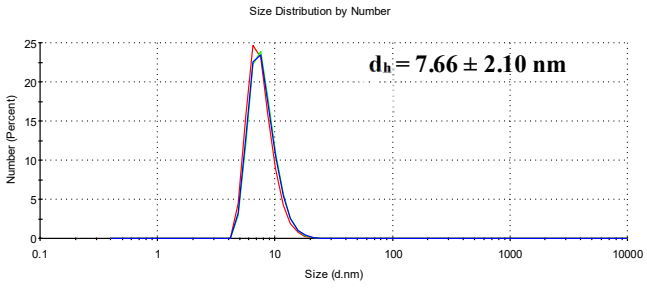

Figure S15. a) Size histogram and b) a representative TEM image; c) TGA and d) hydrodynamic diameter size distribution ± std, n = 3, determined by DLS of **NP2**.

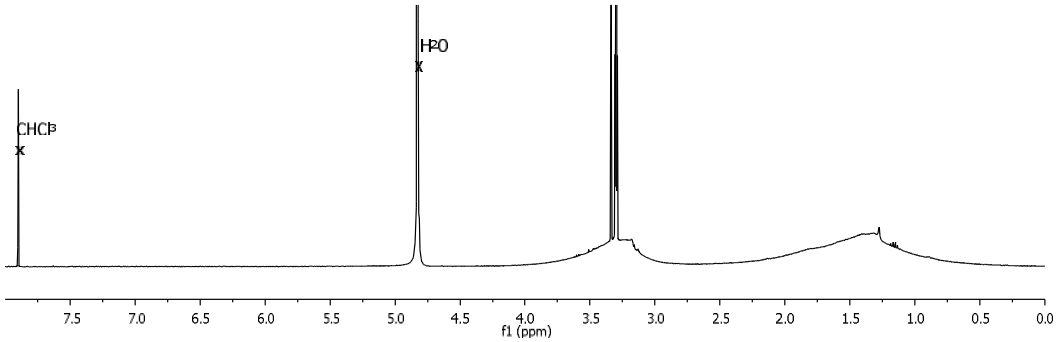

Figure S16. ^{1}H NMR (400 MHz, CD_3OD) spectrum of **NP2**.

4.3 Characterization of NP3

a)

b)

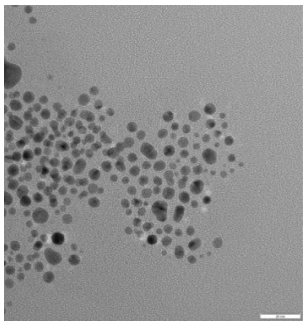

Scale bar: 20 nm

c)

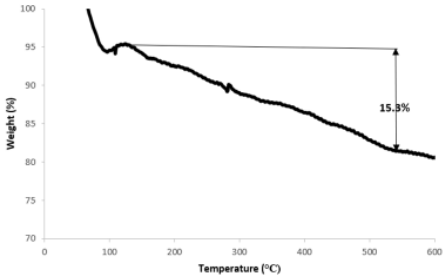

d)

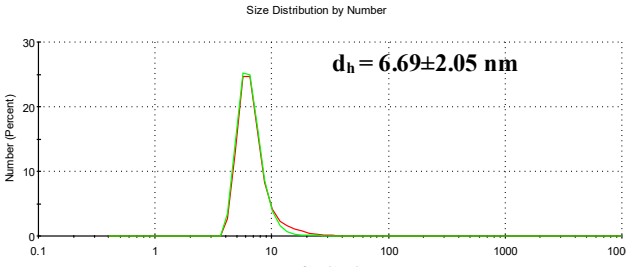

Figure S17. a) Size histogram and b) a representative TEM image; c) TGA and d) hydrodynamic diameter size distribution ± std, n = 3, determined by DLS of **NP3**.

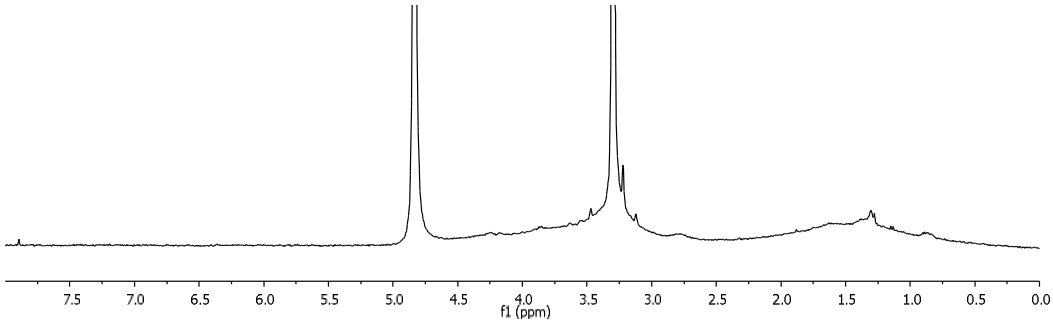

Figure S18. ^{1}H NMR (400 MHz, CD_3OD) spectrum of **NP3**.

4.4 Characterization of NP4

a)

b)

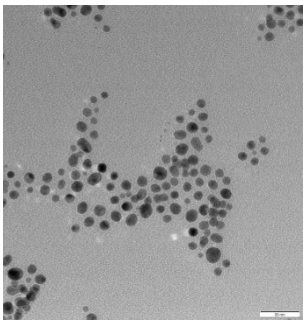

Scale bar = 20 nm

c)

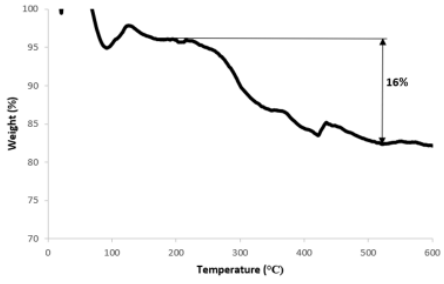

d)

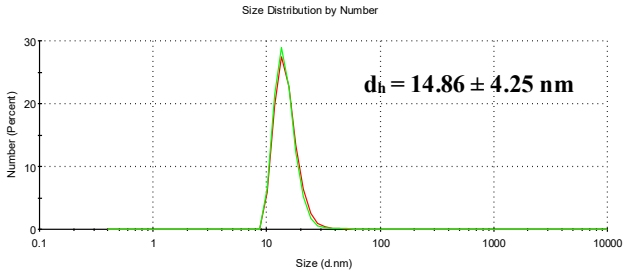

Figure S19. a. Size histogram and b) a representative TEM image; c) TGA and d) hydrodynamic diameter size distribution ± std, n = 3, determined by DLS of **NP4**.

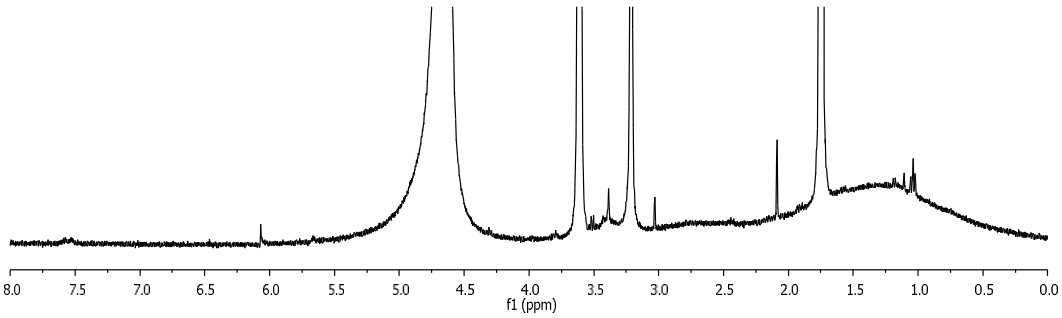

Figure S20. ^{1}H NMR (400 MHz, CD_3OD) spectrum of **NP4**.

4.5 Characterization of NP5

a) b)

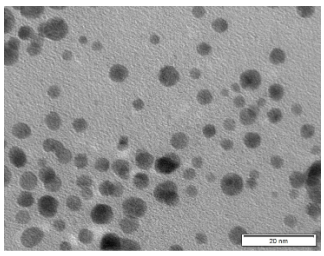

Scale bar = 20 nm

c) d)

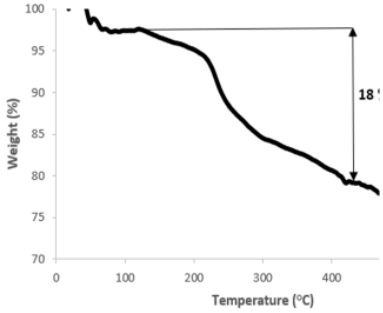

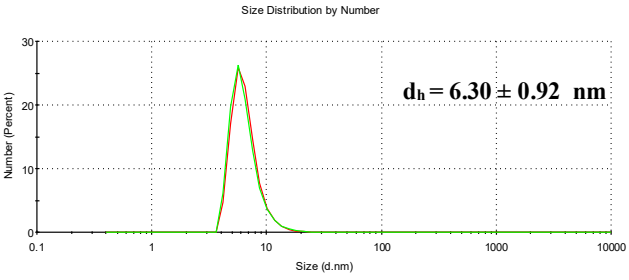

Figure S21. a. Size histogram and b) a representative TEM image; c) TGA and d) hydrodynamic diameter size distribution ± std, n = 3, determined by DLS of **NP5**.

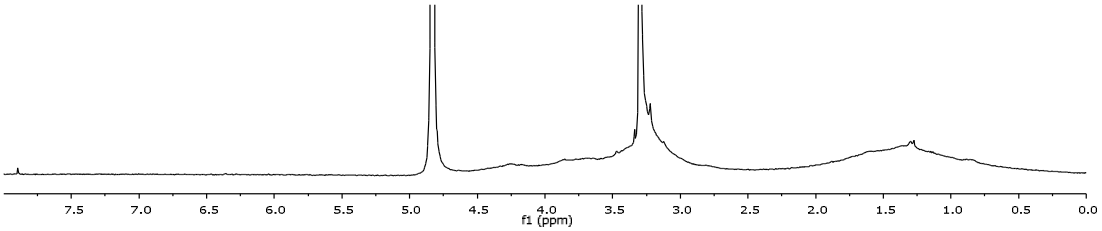

Figure S22. ^{1}H NMR (400 MHz, CD_3OD) spectrum of **NP5**.

4.6 Calculations for the determination of NP composition

From TEM analysis the average NP diameter is determined, d_c. This value is used to calculate the volume of the core considering the NP as a sphere.

$V_c = (\pi/6) \times d_c \text{ nm})^3$

The bulk density ρ_c of Au is 19.3 g/cm^3

The mass of the NP core is: $m_c = \rho_c \times V_c$

The molar mass of NP core is $M_c = m_c \times N_A$ (N_A is the Avogadro number equal to 6.02×10^{23} mol^{-1})

The number of gold atoms, considering the molar mass of Au, M_{Au}, to be 197 g/mol, is: $N_{Au} = M_c/M_{Au}$

From TGA the mass of the organic coating is obtained. The average number of ligands per NP are then calculated considering the number of Au core in the TGA sample and the MW of the thiol as detailed below:

From the total mass of the sample deposited in the TGA pan, m_{NP_pel}, the mass loss from about 100 to 500 °C is attributed to the organic coating, m_{NP,org_pel}, the remaining mass is of the gold core, m_{NP_pel}.

The number of Au core in the sample is: $N_c = m_{NP\_pel}/m_c$

The mass of the coating for each NP is: $m_{NP,org} = m_{NP,org\_pel}/N_c$

The average number of ligand per NP is: $N_{ligand/NP} = m_{NP,org}/MW_{ligand}$

5. XPS Characterization of NPs

Samples **NP2** and **NP5** have been characterized by synchrotron-based x-ray photoelectron spectroscopy (XPS), in order to estimate the thickness of the organic shell around the nanoparticles. The experiments were carried out at the Material Science beamline of the Elettra synchrotron radiation facility in Trieste, Italy. The NPs were dispersed in aqueous solution and then drop casted on a n-doped Si wafer, capped with a layer of native oxide (thickness of the oxide ~4 nm). After drying the samples for 24 hrs in a protected environment in atmospheric pressure, they were inserted in the experimental UHV chamber of the beamline and promptly measured. The base pressure during the experiment was ca. 2×10^{-10} mbar. XPS measurements were carried out by means of a Specs Phoibos 150 analyzer, fitted with a 1D-delay line detector built in house. The overall energy resolution of the experiment was ca. 200 meV. The photoelectrons were collected at a normal emission angle.

The core-level spectra were fitted with Doniach–Sunjic profiles[4] convoluted with a Gaussian function on a linear background, thus obtaining the lineshape parameters, the photoemission intensity, and core-level binding energies (BEs).

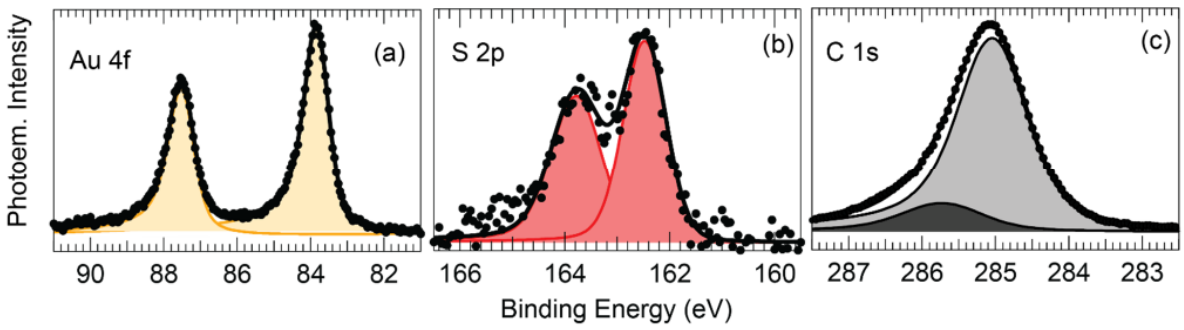

Figure S23: (a) Au 4f, (b) S 2p, (c) C 1s core levels, acquired for sample **NP2**, showed together with their spectral components and global fit. The linear background was removed for clarity.

In Figure S23, we report the Au 4f core level obtained for **NP2**. The Au 4f and C 1s spectra were measured with a photon energy hv=410 eV, while S 2p was measured with a photon energy of hv=360 eV. The binding energy scale was calibrated assigning the main C 1s peak component to 284.9 eV, which corresponds to the C=C bond in the thiol chains.

[4] S. Doniach, M. Sunjic, *J. Phys. C Solid State Phys.* **1970**, *3*, 285-291.

XPS analysis revealed a single Au4f$_{7/2}$ core level component with a BE of 83.9 eV, which is compatible with the presence of Au(0)[5,6]. Similarly, the S 2p shows a spin-orbit doublet with located at BE = 162.1 eV for S 2p$_{3/2}$ (with a spin-orbit splitting of 1.2 eV), consistent with earlier reports.[17] The C 1s core level (Figure S23-c), beside the main component at BE = 284.9 eV associated with the carbon bonds in the thiol chains, displays a component at BE = 285.8 eV, which we associate to C-N bonds present at the tail of ligand **2**.

Earlier works[7-8] have described a straightforward way through which it was possible to extrapolate the thickness of the organic shell surrounding the NP Au core by evaluating the intensity of the C 1s and Au 4f core levels. In this case, according to the methodology described by Shard[19] we obtained a thickness of the organic shell of 1.875 ± 0.100 nm.

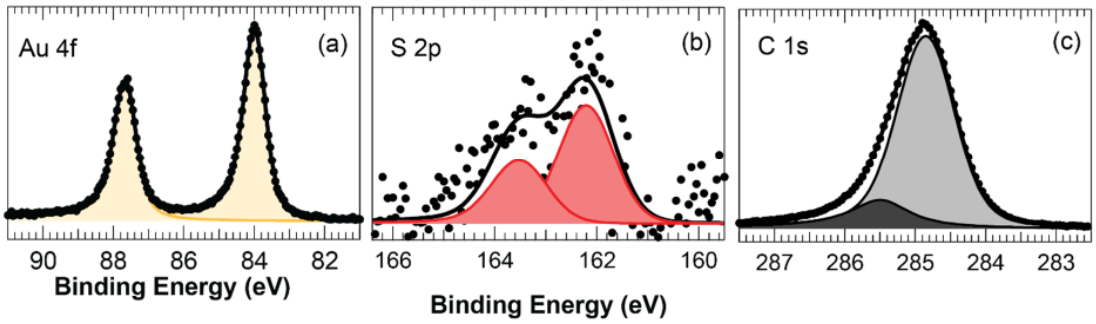

Figure S24: (a) Au 4f, (b) S 2p, (c) C 1s core levels, acquired for sample **NP5**, showed together with their spectral components and global fit. The linear background was removed for clarity.

Similarly, in Figure S24, we report XPS data obtained for the sample **NP5**. The Au 4f$_{7/2}$ core level has a single component at 83.9, indicating also for this sample the presence of Au(0). The thickness of the organic shell surrounding the NP core was found to be 1.372 ± 0.100 nm, which is comparable with the MD computed value of 1.58 nm.

[5] M. J. Hostetler, J. E. Wingate, C.-J. Zhong, J. E. Harris, R. W. Vachet, M. R. Clark, J. D. Londono, S. J. Green, J. J. Stokes, G. D. Wignall, G. L. Glish, M. D. Porter, N. D. Evans, R. W. Murray, *Langmuir* **1998**, *14*, 17-30.
[6] C. Gentilini, F. Evangelista, P. Rudolf, P. Franchi, M. Lucarini, L. Pasquato, *J. Am. Chem. Soc.* **2008**, *130*, 15678–15682.
[7] C. Battocchio, F. Porcaro, S. Mukherjee, E. Magnano, S. Nappini, I. Fratoddi, M. Quintiliani, M. V. Russo, G. Polzonetti, *J. Phys. Chem. C* **2014**, *118*, 8159–8168.
[8] A. G. Shard, *J. Phys. Chem. C* **2012**, *116*, 16806–16813.

6. Simulation details

Table S3. Average number of water molecules, counterions, and equilibrium box lengths (Å) used in the MD calculations for each kind of NP.

System	Water molecules	Counterions	Lx, Ly, Lz
NP1	39579	385 Cl-	111.4 109.6 109.9
NP2	43599	326 Cl-	114.8 115.9 114.9
NP3	36199	330 Na+	107.6 109.3 109.8
NP4	41613	384 Na+	111.6 109.8 110.1
NP5	42657	360 Na+, 360 Cl-	117.7 116.9 120.1
NP6	23203	-	98.6 99.4 96.2